

A method of evaluating and tolerancing interferometer designs

Paul Michaloski, Andrew Kulawiec, Jon Fleig
Tropel Corporation
60 O'Connor Road
Fairport, New York 14450

Abstract

A ray tracing method of simulating interferometers from source to detector using standard optical design software is presented. The advantages, disadvantages and limitations of the method are discussed. The method is applied to the analysis of a phase measuring interferometer designed to test the form of cylindrical mechanical parts and the predicted performance is compared with experimental results.

Introduction

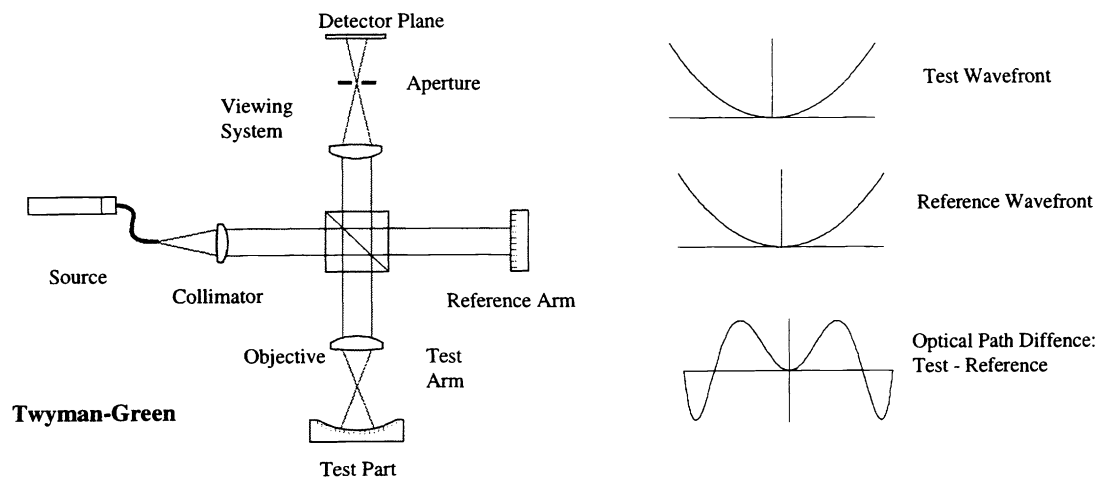
The design of optics for interferometers is commonly accomplished with standard design software by modeling source feeds, objectives, and viewing systems as separate entities. However, the effects of perturbations such as alignment errors, optical fabrication errors, thermal effects, and propagation errors due to non-null test surfaces may be calculated more accurately by simulating the complete interferometer from source to detector. Optical design programs make it easy to introduce perturbations into the simulations. However, such software is strongly oriented toward the design of imaging systems, while the design of a complete interferometer is not primarily an imaging problem. To take advantage of the ease of modeling perturbations with a standard design code, we have developed a straightforward method for using its raw ray trace data to evaluate the non-imaging (phase measurement) characteristics of interferometer designs.

Comparison of Methods

Analyzing interferometer designs requires determining optical path descriptions of the test and reference wavefront profiles in the coordinates of the detector plane. These descriptions are then subtracted to obtain a representation of the phase difference being measured at the detector plane. The wavefront descriptions can be determined either by algebraic or by numerical methods. Algebraic modeling quickly becomes cumbersome when trying to describe real world

optics or complex geometries. Alternatively, wavefront modeling has many advantages, including being able to examine effects of diffraction at apertures or features of the part under test. This also becomes difficult quickly, especially when examining the many different types of perturbations to the optical system needed in tolerancing. On the other hand, ray tracing to determine wavefronts with standard design programs, which is a numerical approach to the problem, has the advantage of being able to model complex systems and to perturb them with ease.

Figure 1



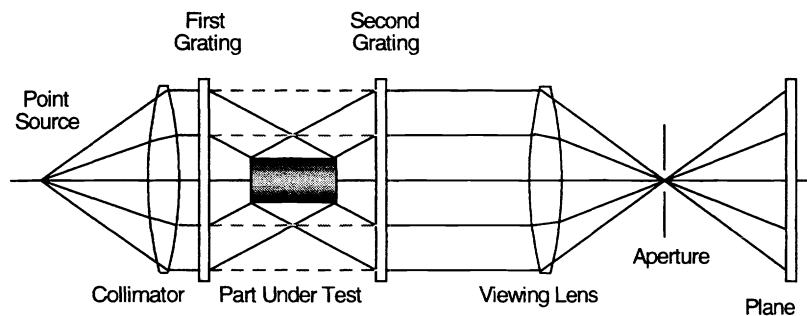
There are a few possibilities for obtaining the wavefront descriptions from ray tracing data at the detector plane. One is to use ray aiming algorithms for sending the rays forwards or backwards from the detector plane. However, increasing the accuracy of the ray aiming algorithm decreases the speed of the tracing. A much more serious problem with ray aiming is that the algorithms become unstable with the addition of more complex optics, such as binary optics, anamorphic optics or lens arrays. A second ray tracing technique is to trace a great number of rays and to bin them into each pixel at the camera. Douglas et al.¹ developed this method for the simulation of an astronomical interferometer using a diffraction grating for examining spectrums. This method is ideal for simulating complex sources, but has the disadvantages of requiring a tremendous number of rays, and in some cases, the development of a whole new ray tracing package. A third method of obtaining descriptors in the coordinates of the detector plane is to fit the two wavefronts into polynomial forms that are easily subtracted. This method is referred to by Noecker et al.² in presenting the tolerancing of a starlight interferometer; unfortunately only a brief discussion of the method was provided.

The “Shotgun” Method

Description:

We refer to the fitting method that we use as a “shotgun” ray trace analysis because the rays are not aimed and their coordinates in the entrance pupil, at the surface under test or at the final image plane are not critical. The rays are traced from some common surface or point at the source to the detector plane for both the reference and the test path. The only information collected from each ray is the optical path length of the ray and the final spatial coordinates at the image plane: (x, y, opl) . Fitting both sets of trace data provides equations for the optical path as a function of position on the image plane: $opl = f(x,y)$. Subtracting the reference and test equations provides the optical path difference in the coordinates of the detector plane: $OPD(x,y) = opl_{test} - opl_{reference}$.

Figure 2



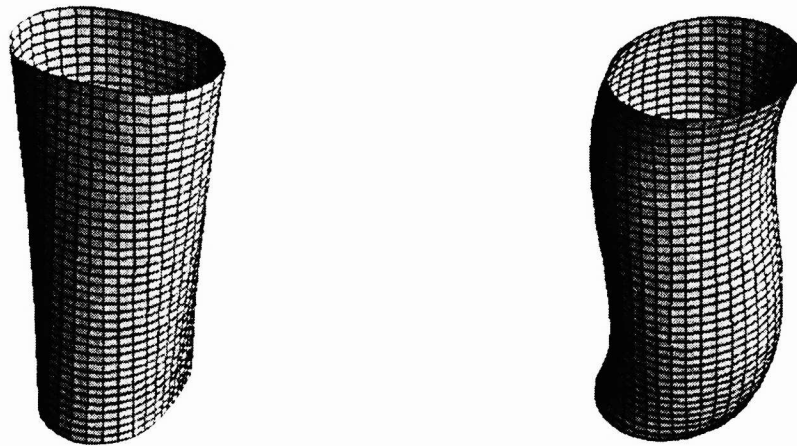
The interferometer shown in figure 2 is for measuring the geometric form error of cylindrical parts.^{3,4} The test and reference paths are differentiated by the diffracting orders of the gratings. The first order is used as the test wavefront (solid lines) and the zero order as the reference (dash lines). The two gratings are concentric circular, constant pitch binary gratings. The second grating is translated to modulate fringes for phase measurement. The inside of cylindrical parts can also be measured with the first order of opposite sign.

Fitting the Wavefronts:

The shape of the surface under test and its projection at the image plane determines the equational form to fit to the ray data. The use of an orthonormal polynomial avoids accuracy of the fitted terms being dependent on the number of terms in the fit. Also, the terms often provide more meaningful interpretations to the perturbations to the system. Zernike polynomials are the obvious choice for an interferometer measuring a surface that is projected to a circle. In the case

of interferometer measuring a cylinder projected to an annulus, a different set of orthonormal polynomials is chosen. This set consists of Legendre polynomials for variations along the length of the cylinder and sinusoidal functions (Fourier components) for variations of roundness.⁵ Interferometric test and reference wavefront profiles can contain a great amount of piston, tilt and/or power that are common to both. We have found that the fitting process is best performed in two stages. The first is to remove the common low order terms of piston, tilt and power. The second is to fit the residual of both the test and reference after their removal

Figure 3



2 lobe • twist : $z \cos(2\theta)$

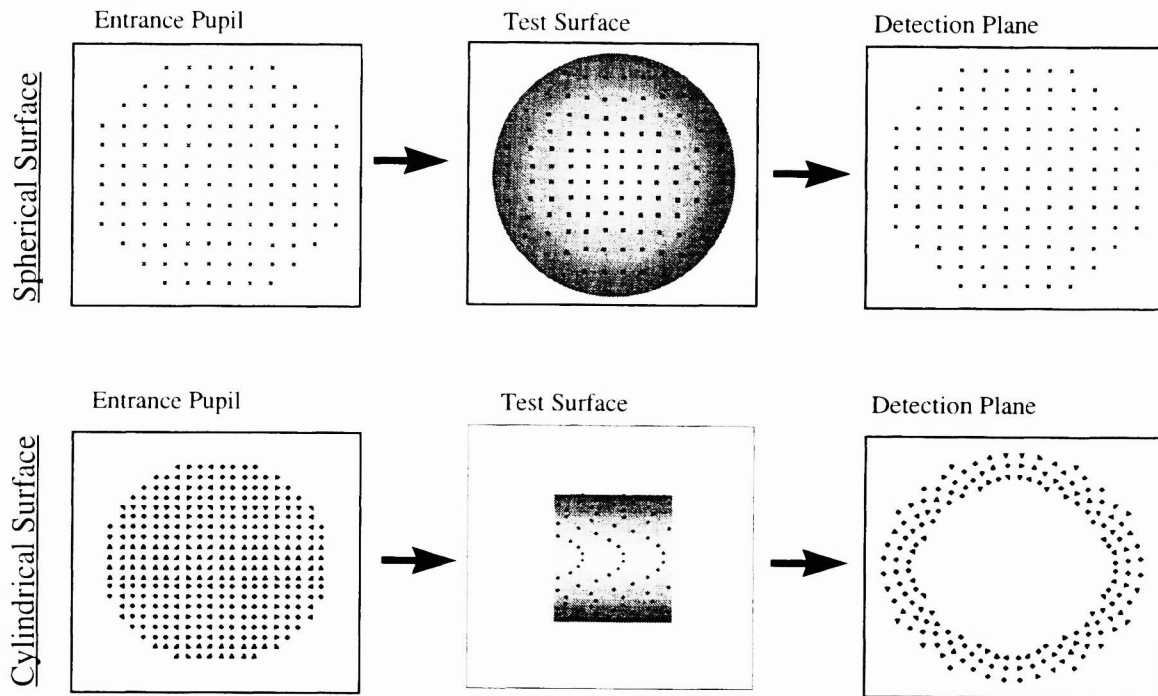
2 hump • tilt: $\frac{(5z^3 - 3z)}{2} \cos(\theta)$

where z is along the length and θ is the azimuth angle

Sampling Density and Boundary Determination:

Fitting ray data to orthonormal polynomials requires that the coordinates of the intercepts be normalized to some defined aperture or boundary. In the case of Zernikes, the boundary is a circle whose center and radius need to be defined. In the case of the Fourier-Legendre polynomials for cylinders, the annulus needs center and both an inner and outer radius. This boundary is the outline of the projection on the detector plane of the surface under test. While the position of the rays at the surface of the part are not critical, nor tracked, they are important in terms of sampling and determining the boundary.

Figure 4



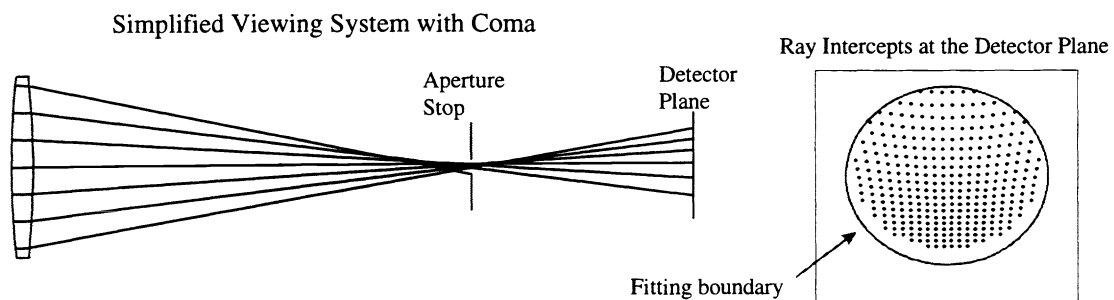
Since only rays reflecting off the part will successfully pass through the system, the boundary of the fitting can be determined by the coordinates of the set of test rays at the detector plane. Of course, this is limited by how close the rays approach the edge of the surface under test. As an example, a circle of an unknown diameter that is nearly inscribed to a 64x64 square grid of points will have a point inside the circumference to within at least 0.25% of the radius. This indicates that a 64x64 grid of rays traced into the entrance pupil should be able to determine the diameter of the part to 0.25%. Increasing the density of rays traced into the entrance pupil of the system increases both the accuracy of the boundary definition and the sampling of the part and all of the other optics in the interferometer. Insufficient sampling could lead to erroneous results. In setting up the simulation, it is simple to check the adequacy of the sampling by increasing the density of rays until the results do not vary significantly.

Limitations:

The viewing system of an interferometer needs an aperture stop in order to filter out sources of spurious fringes of high spatial frequency. In terms of the simulation, higher spatial frequency components cause high deviations of slope in the wavefronts. The ray sampling and the aperture stop limit the spatial frequency of perturbations that can be examined in the shotgun simulations. During the simulation, if a region of the detector is being shadowed (i.e. rays are blocked) by the

aperture stop of the viewing system, the fitting algorithms could produce an erroneous result based on the rest of the detector. The region missing ray data would not be evident in the final phase map. Such erroneous results are easily avoided by keeping track of the number of rays passed. The number of rays passing a perturbed system should be nearly identical to that of a nominal, or un-perturbed system. Misalignments, which are of a low spatial frequency, could also force the rays outside the viewing system aperture. In the initial setup of the interferometer the aperture is aligned to the observed focus. This alignment procedure can be taken into account when determining the tolerances of the setup alignments by having the aperture automatically aligned to the center of the ray intercepts at the aperture plane. This is easily automated in optical design programs with user programming capabilities.

Figure 5



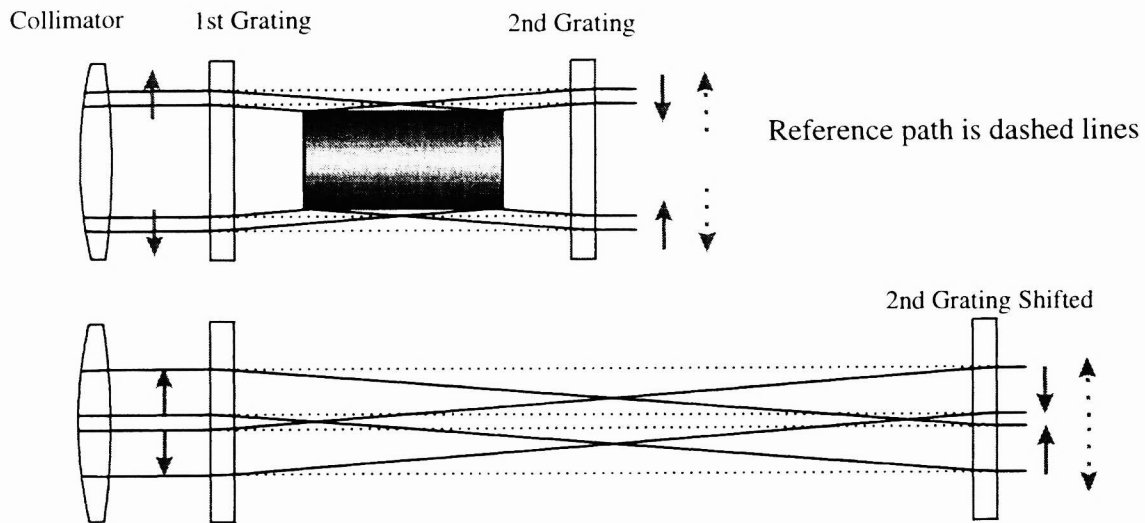
Tracing through the viewing system of the interferometer plane allows one to take into account propagation and design factors that can distort the image of the surface under test. Once again, the magnitude of wavefront slope errors that distorts the wavefront with propagation can be simulated is limited. This is due to sampling, the rays passing the system and also the degree in which the mapping of the part to the detector plane is continuous. If the part is being imaged well by the viewing system, it is continuous and perturbations to the surface under test should not alter the mapping of the part. In fact, one means of evaluating the imaging performance of the viewing system is to examine the variations in correlation between the perturbations of the part and the simulated measurements. Image distortion can be evaluated by examining the correlation of a simulated measurement and an un-perturbed part. These evaluations of the viewing system are useful but do not tell all. For example, a simulated measurement with a detector plane shifted out of focus would only change due to distortion in the imaging. An actual measurement with defocus would lose information at the perimeter of the part being measured due to edge diffraction (Fresnel rings).

Examples

Aberrated Collimator:

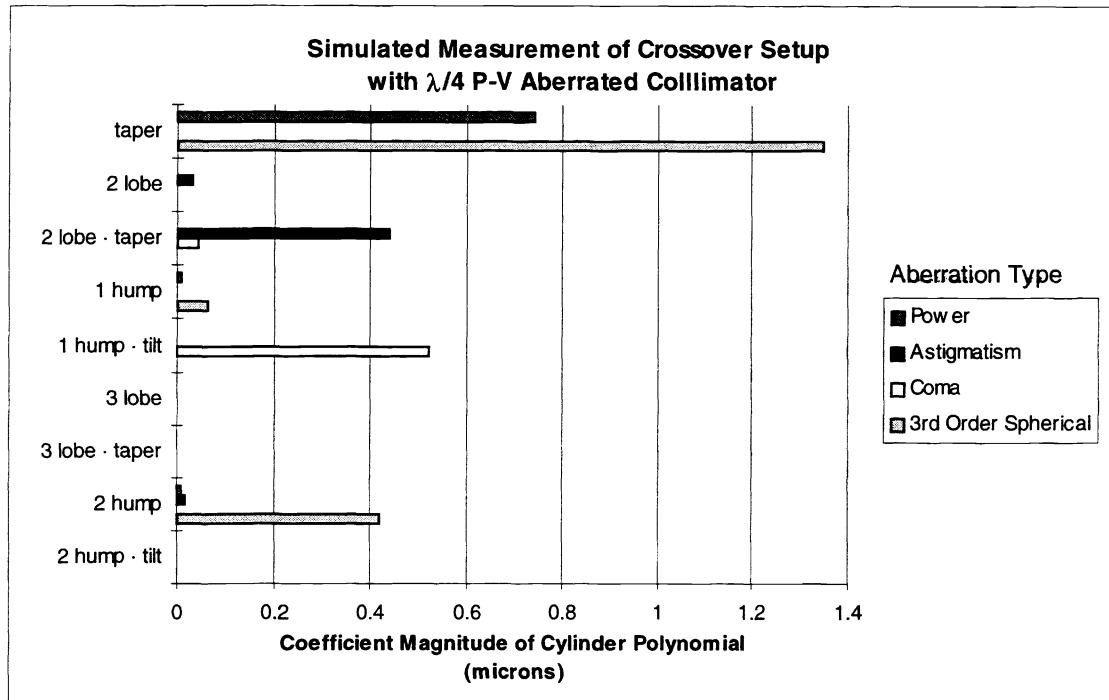
In many interferometers the effects due to aberrations of the collimator or source feed optics is minimal due to the test and reference sharing the same path. In the case of the cylinder measuring interferometer the test wavefront is turned inside out by the reflection at the cylinder.

Figure 6



This guarantees that the test and reference wavefronts will not traverse the same path of the collimator at the plane of the 2nd binary optic. In fact, the portion of the collimator that is traversed by the two paths are dependent on the dimensions of the cylinder and whether an inner or outer surface is being measured. A more general case of the test wavefront crossing over the optical axis arises when no part is present. This configuration may be used to analyze the collimator aberrations. In order to understand how to interpret the results of a crossover measurement, a set of simulations was run with perturbed collimator wavefronts. The collimator was perturbed, one by one, with a quarter wave P-V of power (decollimation), astigmatism, coma and spherical aberration.

Figure 7



The results, summarized in figure 7, show that each of the collimator's aberrations has its own signature in terms of the Fourier-Legendre polynomials. A similar analysis with various part sizes was used to determine the needed performance specification for the collimating optics.

Correlation with Measurement:

The perturbation chosen for the comparison of measurement and simulation is to decenter the source, which is a fiber optic feed. The source was decentered laterally in two steps of 25 μm while measuring the outer diameter of an 8 mm φ by 28 mm length cylinder. The significant terms of the measurements and the shotgun simulations are compared in Table 1.

Table 1

	Simulation			Measurement			Meas./Simulation	
	25 μm (μm)	50 μm (μm)	50/25 ratio	25 μm (μm)	50 μm (μm)	50/25 ratio	25 μm ratio	50 μm ratio
tilt	7.182	14.469	2.0	7.360	15.376	2.1	1.02	1.06
2 lobe	0.054	0.214	4.0	0.057	0.264	4.8	1.07	1.24
taper	0.016	0.064	4.0	0.023	0.093	4.0	1.47	1.45
2 lobe · taper	0.016	0.063	4.0	0.014	0.054	4.1	0.90	0.85

Tilt is the most significant result of the perturbation and varies linearly with the decentration. The remaining terms are two orders of magnitude smaller and have a quadratic dependence with decentration. Off axis, the collimator is dominated by astigmatism, so it is no surprise that '2 lobe' is the largest of the non-alignment terms.

Summary

A method of tolerancing and evaluating interferometer designs with the use of standard optical design programs has been described and demonstrated for a cylindrical form measuring interferometer. This method can examine a complete interferometer from source to detector, and is quick and robust enough for use in extensive tolerancing. It is best suited for examining perturbations that produce small slope errors to the wavefronts, such as most misalignments, optical fabrication errors and thermal effects.

Acknowledgments

We would like to thank Bill Castle for providing measurements and Tim Rich for his help on the presentation of the orthonormal polynomials.

References

- ¹ N. G. Douglas, A. R. Jones, F. J. van Hoesel, "Ray-based simulations of an optical interferometer", *J. Opt. Soc. Am. A* **12**, 124-131 (1995)
- ² M. Charles Noecker, Marc A. Murison, Robert D. Reasenberg, "Optic-misalignment tolerances for the POINTS interferometer", *SPIE Vol. 1947 Spaceborne Interferometry*, 218-231 (1993)
- ³ Thomas Dresel, Johannes Schwider, Alexander Wehrhahn, Sergey Babin, "Grazing incidence interferometry applied to the measurement of cylindrical surfaces", *Optical Engineering* **34**(12), 3531-3535 (1995)
- ⁴ John H. Bruning, "Interferometric measurement of surfaces with diffractive optics at grazing incidence", U.S. Patent 5,654,798
- ⁵ P. Glenn, "Set of orthonormal surface error descriptors for near-cylinder optics", *Optical Engineering* **23**(4), 384-390 (1984)